
Supplementary material to:

What surface radiative fluxes reveal about Arctic cloud modelling accuracy

Yaël Le Gars¹, Jean-Christophe Raut¹, Louis Marelle¹

¹LATMOS/IPSL, Sorbonne Université, UVSQ, CNRS, Paris, France

This document provides additional figures and tables supporting the main manuscript.

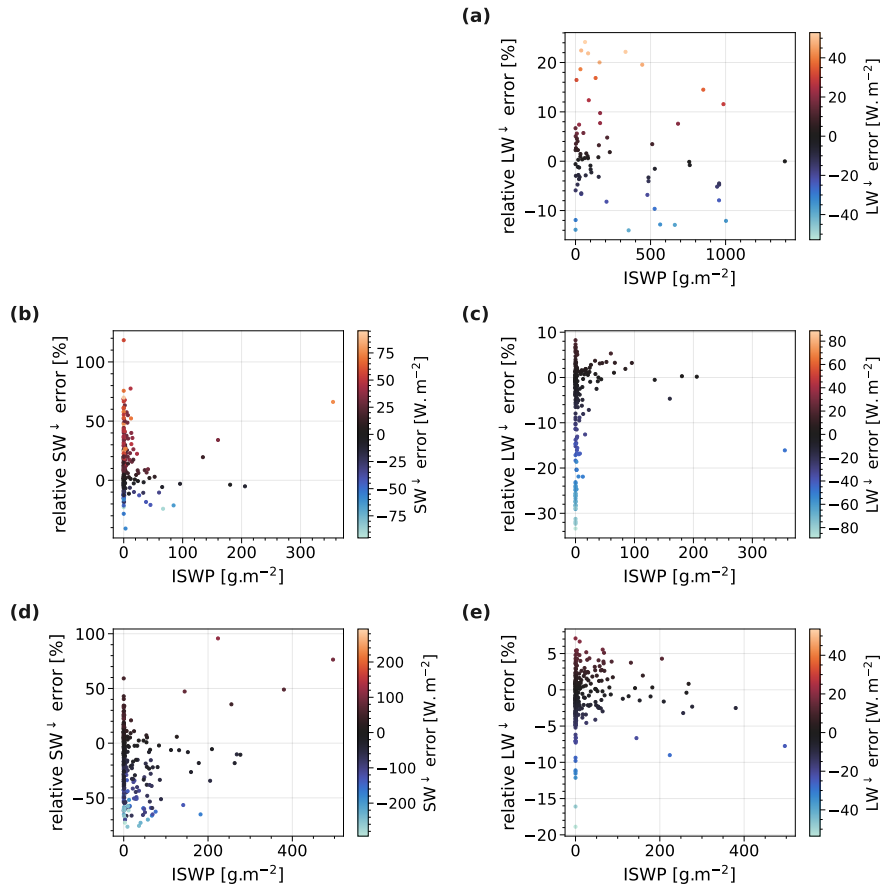


Figure S1: Radiative fluxes biases as a function of modelled ice and snow water path (ISWP), showing relative error (model minus observation) on y-axis and colour-coded by the raw error. (a) LW[↓] errors during P1, (b) SW[↓] errors during P2, (c) LW[↓] errors during P2, (d) SW[↓] errors during P3 and (e) LW[↓] biases during P3.

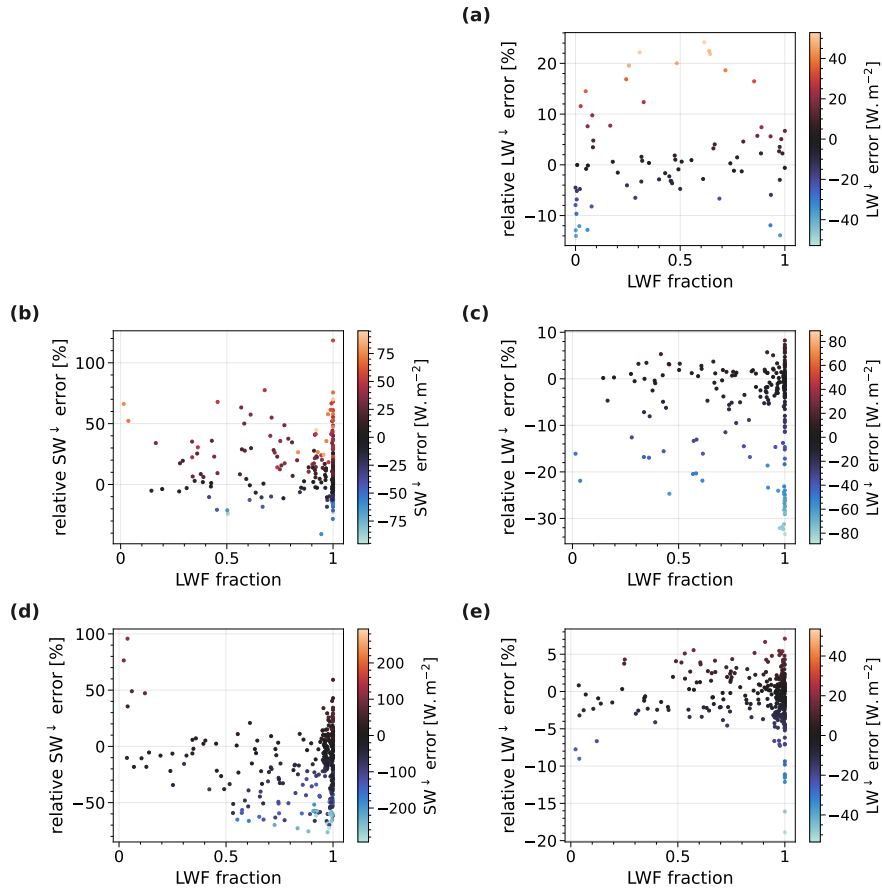


Figure S2: Radiative fluxes biases as a function of modelled liquid water fraction (LWF), showing relative error (model minus observation) on y-axis and colour-coded by the raw error. (a) LW^\downarrow errors during P1, (b) SW^\downarrow errors during P2, (c) LW^\downarrow errors during P2, (d) SW^\downarrow errors during P3 and (e) LW^\downarrow biases during P3.

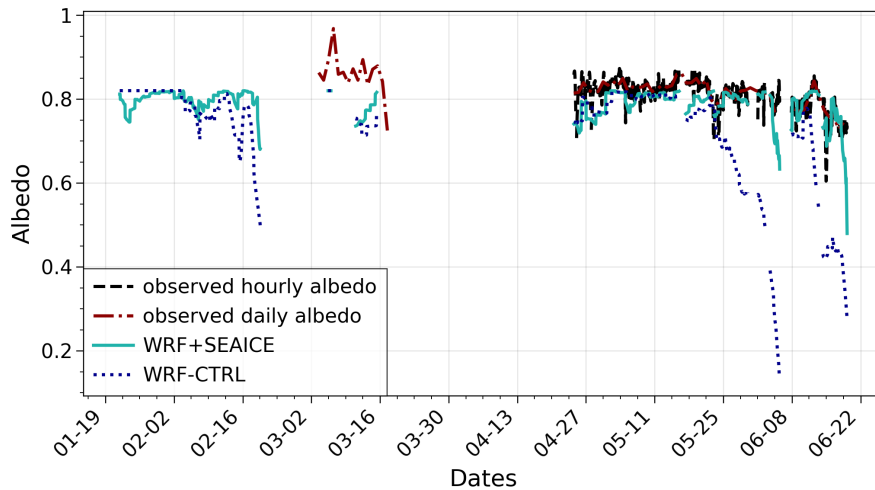


Figure S3: Temporal serie of observed (daily and hourly) and modelled (WRF-CTRL and WRF-SEAICE) hourly surface Albedo. Observed daily albedo is provide by N-ICE measurements at noon. Observed hourly albedo is calculated as the ratio of hourly measured SW^\uparrow/SW for comparison.

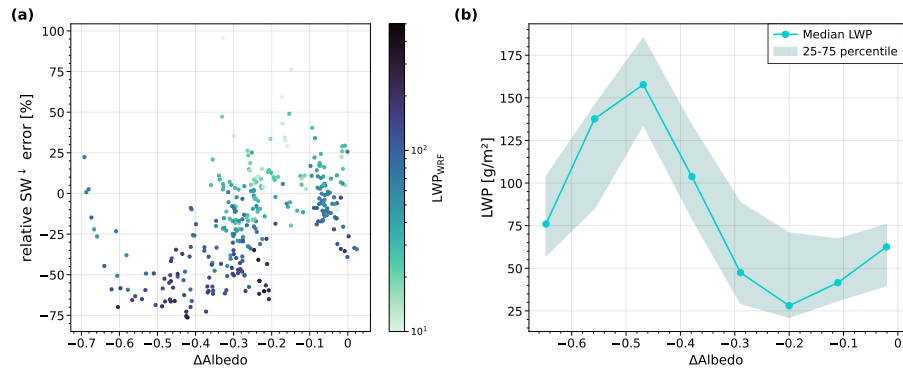


Figure S4: **(a)** P3 SW[↓] errors distribution as a function of surface albedo biases with LWP_{WRF} colored during. **(b)** binned LWP values distribution with respect to surface albedo biases.

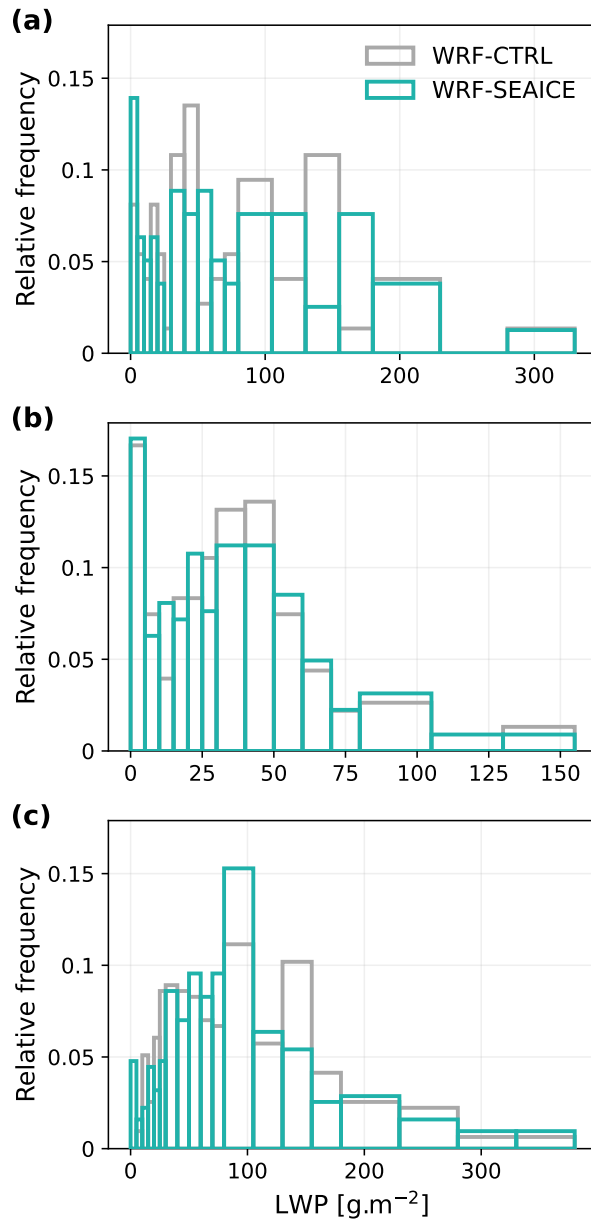


Figure S5: Adaptive binned distribution of LWP values, comparing WRF-CTRL and WRF-SEAICE for a) P1, b) P2 and c) P3. Bin size of $5 \text{ g}\cdot\text{m}^{-2}$ when $\text{LWP} \leq 30 \text{ g}\cdot\text{m}^{-2}$, 10 when $\text{LWP} \leq 80 \text{ g}\cdot\text{m}^{-2}$ and 25 otherwise.

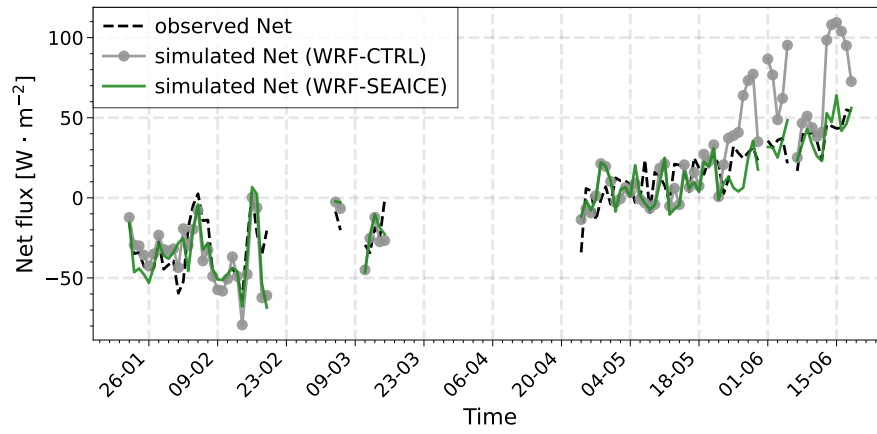


Figure S6: Time series of observed (dashed black) and simulated net radiation from WRF-CTRL (dotted gray) and WRF-SEAICE (solid green) along the N-ICE drift.

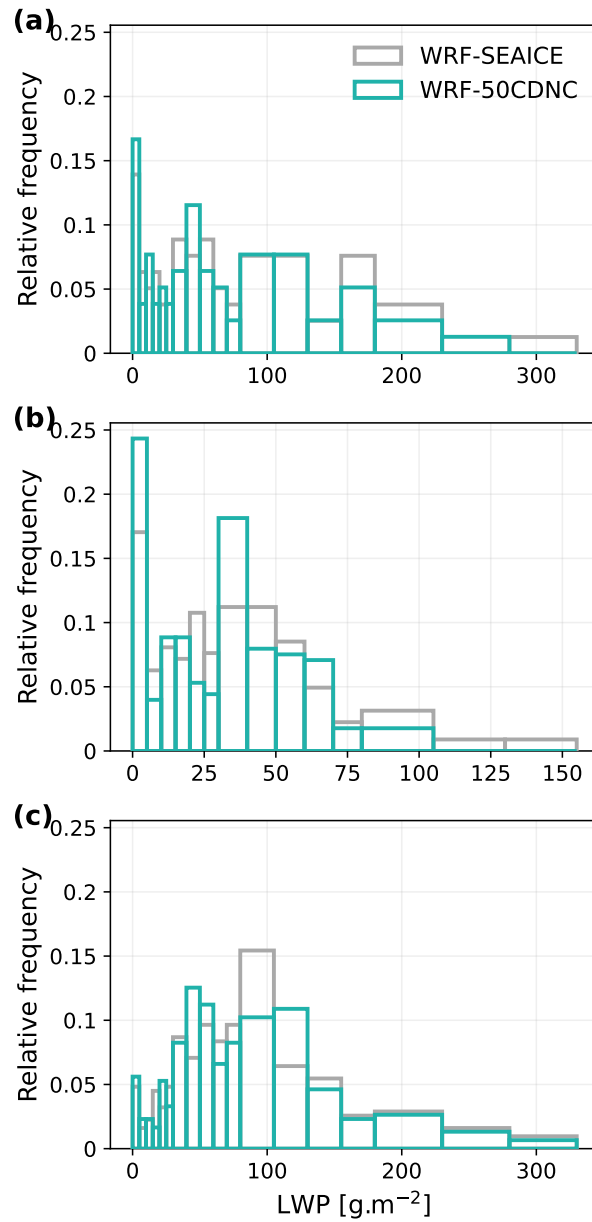


Figure S7: Adaptive binned distribution of LWP values, comparing WRF-SEAICE (100 CDNC) and WRF-50CDNC for a) P1, b) P2 and c) P3. Bin size of 5 g.m^{-2} when $\text{LWP} \leq 30 \text{ g.m}^{-2}$, 10 g.m^{-2} when $\text{LWP} \leq 80 \text{ g.m}^{-2}$ and 25 otherwise.

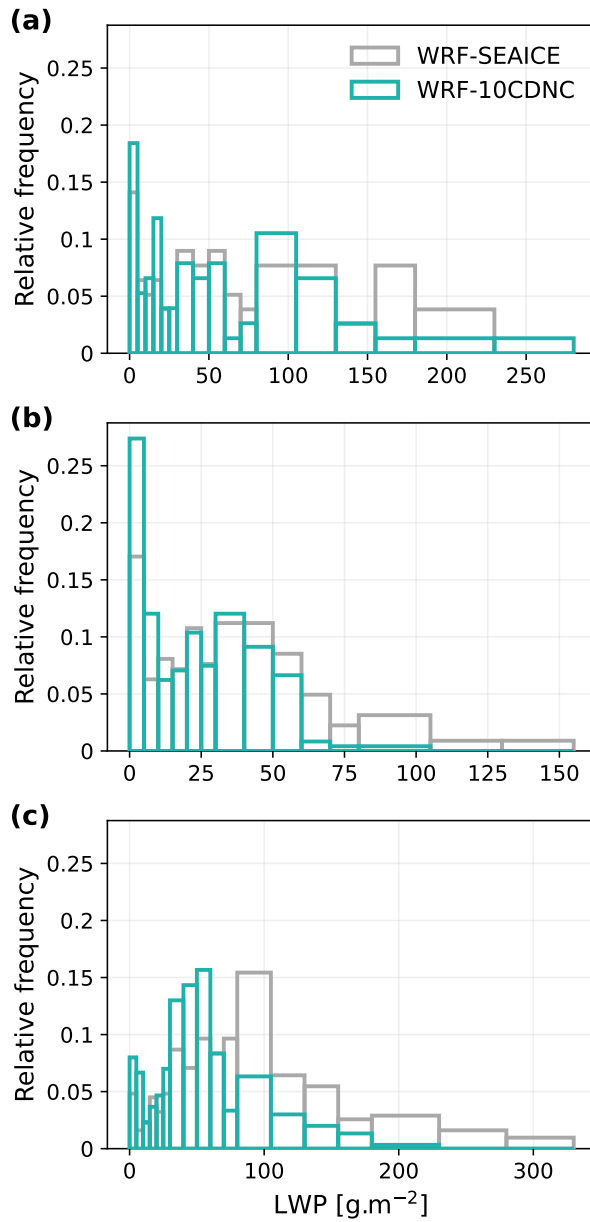


Figure S8: Adaptive binned distribution of LWP values, comparing WRF-SEAICE (100 CDNC) and WRF-10CDNC for a) P1, b) P2 and c) P3. Bin size of 5 $\text{g}\cdot\text{m}^{-2}$ when $\text{LWP} \leq 30 \text{ g}\cdot\text{m}^{-2}$, 10 when $\text{LWP} \leq 80 \text{ g}\cdot\text{m}^{-2}$ and 25 otherwise.